

Inclusive searches for squarks and gluinos with the ATLAS detector

S. Adachi^{1,a}, on behalf of the ATLAS Collaboration

¹*The University of Tokyo, 7-3-1 Hongo, Bunkyo-ku, Tokyo, Japan*

Abstract. Despite the absence of experimental evidence, the weak scale supersymmetry remains as one of the best motivated and studied theoretical models beyond the Standard Model. This article summarises recent ATLAS results on inclusive searches for squarks and gluinos in R-parity conserving SUSY scenarios, including third generation squarks produced in the decay of gluinos. The searches involve final states containing jets, missing transverse momentum with and without a light lepton. No significance excess above the Standard Model prediction is observed and exclusion limits are set on 2-dimensional mass planes of benchmark signal models.

1 Introduction

Supersymmetry (SUSY) [1–6] is one of well-motivated Standard Model (SM) extensions, and it predicts new bosonic partners for the fermions and new fermionic partners for the bosons of the Standard Model. If R-parity is conserved [7], SUSY particles are produced in pairs and the lightest supersymmetric particle (LSP) is stable and represents a possible dark-matter candidate. The scalar partners of the quarks, squarks (\tilde{q}), and the fermionic partners of the gluons, gluinos (\tilde{g}), could be produced in strong-interaction processes at the Large Hadron Collider (LHC) and decay to the stable LSP, which is undetectable, producing substantial missing transverse momentum (p_T^{miss}).

Recent ATLAS [8] results use the data recorded in 2015 and 2016 in $\sqrt{s} = 13$ TeV proton-proton collisions at the LHC, corresponding to an integrated luminosity of 36.1 fb^{-1} . There are various squarks and gluinos searches based on topology in the final state aiming to cover all possible decay chains. Our searches consider various cascade decays including direct, one-step and two-step decays as shown in Figures 1–3. The ‘0-lepton (2–6 jets)’ analysis [9] is based on event topology with 2–6 jets, aiming at squarks or gluinos with direct or one-step decay via charginos. The benchmark signals are shown in Figure 1. In these signals, the gluino and squark are modeled in the simplified model [10–12], in which the gluino and squark decay via virtual light-flavour squarks. Hence no bottom or top quarks are produced in the final states. The ‘0-lepton (7–11 jets)’ analysis [13] is based on event topology with 7 or more jets, targeting gluino pair-production with one-step or two-step decay via charginos or the second lightest neutralinos (Figure 2). The one-step decay predicted in a scenario of the phenomenological Minimal Supersymmetric Standard Model (pMSSM) [14, 15] has high jet-multiplicity caused by the decays of top quarks and other bosons appearing in the decay chains. The two-step decay in the simplified model has high jet-multiplicity caused by these long decay chains.

^ae-mail: shunsuke.adachi@cern.ch

The '1-lepton' analysis [16] is based on event topology with one isolated lepton (electron or muon) and jets, in which there are 3 categories with different jet multiplicities. Categories with at least 2 jets, 4–5 jets and at least 6 jets are aiming at squark and gluino pair-productions with one-step decay in Figures 1b and 1d, and the category with at least 9 jets is designed for higher jet-multiplicity signals as shown in Figure 2. The last analysis is "multi-*b*" analysis [17], which is prepared for special cases of gluino direct decays that have many bottom quarks in final states as shown in Figure 3, and requires multi *b*-quark jets in the selection. These signals are well-motivated because stop or sbottom mass could be relatively lighter than the other light-flavour squarks due to 'naturalness' and gluino could decay via off-shell stop or sbottom to top or bottom quarks. A summary of the signal topology in these 4 analyses is given in Table 1.

Table 1: Coverage of each analysis searching for squarks or gluinos production.

Decay process	Direct decay	One-step decay	Two-step decay
0-lepton		0-lepton (2–6 jets) [9]	0-lepton (7–11 jets) [13]
1-lepton	-		1-lepton (2–6 jets, 9 jets) [16]
<i>b</i> -quarks	Multi- <i>b</i> [17]	-	-

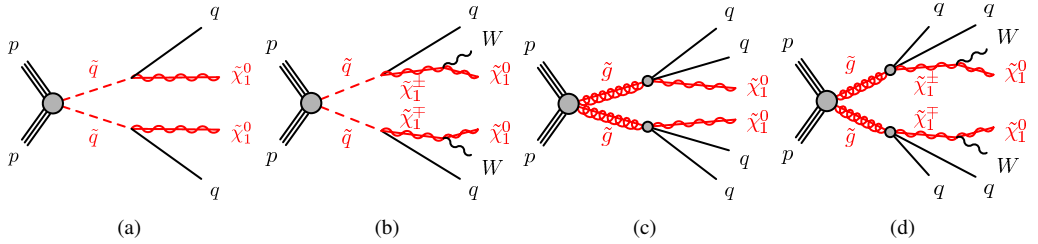


Figure 1: The decay topologies of (a) (b) squark pair production and (c) (d) gluino pair production in the simplified models with direct decays (a) (c) or one-step decays (b) (d).

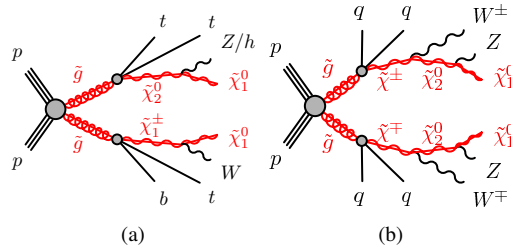


Figure 2: The decay topologies of gluino pair production in (a) the pMSSM scenario with one-step decay and (b) the simplified model with two-step decay.

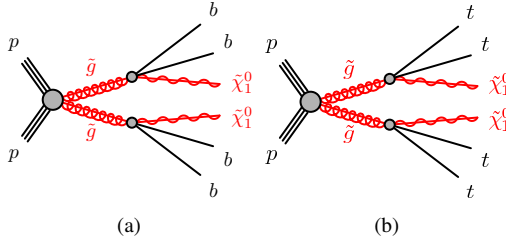


Figure 3: The decay topologies of gluino pair production in the simplified models with direct decay to neutralinos and (a) b -quarks or (b) top-quarks via off-shell sbottom or stop.

2 0-lepton (2–6jets) and 1-lepton (2–6jets) analyses

2.1 Signal region definitions and background estimation

In these analyses, the powerful discriminating variable between signal and SM background is 'effective mass', m_{eff} , that is scalar sum of $E_{\text{T}}^{\text{miss}}$ and p_{T} s of all jets and leptons, where $E_{\text{T}}^{\text{miss}}$ is the magnitude of the transverse missing momentum ($p_{\text{T}}^{\text{miss}}$). Signal regions (SRs) are defined to enhance the expected signal yield relative to the SM backgrounds. Because the effective mass is strongly correlated to masses of SUSY particles, the SRs with various effective mass cuts need to be prepared in order to cover the wide mass ranges. To estimate the SM backgrounds, control regions (CRs) are defined for each of the SRs. They are chosen to be orthogonal to the SR selections in order to provide independent data samples enriched in particular backgrounds, and are used to normalize the background MC simulation. Cross-checks of the background estimates are performed with data in several validation regions (VRs) selected with requirements such that these regions do not overlap with the CR and SR selections. These CRs and VRs have a low expected signal contamination.

2.2 Results and interpretation

To extract the final results, two kinds of likelihood fits are employed: background-only and model-dependent fits. A background-only fit is used to estimate the background yields in each SR. The fit is performed using the observed event yields in the CRs associated with the SR as the only constraints, but not using the yields in the SR itself. It is assumed that signal events from physics beyond the Standard Model (BSM) do not contribute to these CR yields. The scale factors represent the normalization of background components relative to MC predictions, and are determined in the fit to all the CRs associated with a SR.

A model-dependent fit is used to set exclusion limits on the signal cross-sections for specific SUSY models. The fit proceeds in the same way as the background-only fit, where yields in the CRs are used to constrain the predictions of backgrounds in each SR, while the SR yield is also used in the likelihood.

The results of background-only fits are shown in Figures 4a and 4b. Figure 4a shows SRs with various number of jets selections and m_{eff} cuts in 'Meff-based searches' in the 0-lepton analysis. Meff-based searches use a conventional variable of m_{eff} as a discriminating variable. In addition to them, R-jigsaw-based searches are performed, which use new variables obtained from "Recursive Jigsaw Reconstruction" technique [18–20]. This technique can improve the sensitivity especially for the

signals with small mass difference between squark or gluino and LSP. In the both searches, there is no significant excess. Figure 4b shows the SRs in the 1-lepton analysis including at least 9jets regions described in Section 3. There is no significant excess in all of the SRs.

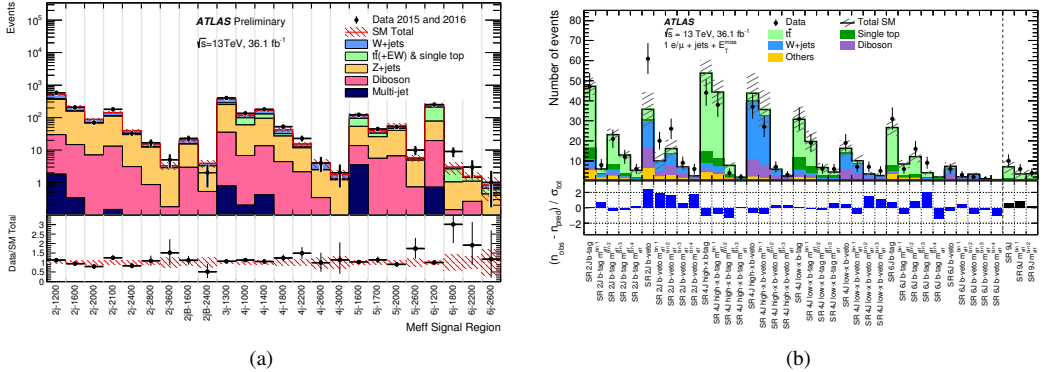


Figure 4: Comparison of the observed data and predicted background event yields in (a) signal regions of the 0-lepton (2–6jets) analysis [9], and (b) signal regions of the 1-lepton analysis [16]. Each bin indicates a yield in one signal region. The bottom panel in Figure (a) shows the ratio of observed data yields to the total predicted background yields, and that in Figure (b) shows the difference between the observed data yields and the predicted total background yields divided by total uncertainties. The regions in Figure (b) are all of the signal regions in the 1-lepton analysis including at least 9jets regions described in Section 3.

Since there is no excess, the model-dependent fits are performed for the benchmark signal models. The fit results are interpreted in 2 dimensional mass planes. Figure 5 shows interpretation of the 0-lepton (2–6jets) analysis on squark- or gluino-LSP mass planes in the direct decay signals. Figures 6 and 7 show interpretations of the 0-lepton (2–6jets) and the 1-lepton analyses on the same 2 dimensional mass plane in one-step decay signals of squark and gluino pair-production, respectively. The contours present expected and observed 95% CL exclusion limits. In the 0-lepton analysis, the limits are obtained by using the SR with the best expected sensitivity at each mass point in Meff- and R-jigsaw-based searches. In the 1-lepton analysis, the limits are obtained by a model-dependent fit over all of the 2–6jets SRs. The squark mass is excluded up to 1.6 TeV and 1.2 TeV in the cases of direct decay and one-step decay, respectively. The gluino mass is excluded up to 2.0–2.1 TeV in both cases.

3 0-lepton 7–11jets and 1-lepton (9jets) analyses

3.1 Signal regions and background estimation

The 0-lepton (7–11 jets) analysis and 9 jets SRs in the 1-lepton analysis are aiming at the signals with high jet-multiplicity. SRs with various jet-multiplicities and various bottom quark multiplicities are prepared to cover various signal decays. An accurate modeling of high jet-multiplicity processes from QCD calculations and matrix-element MC event generation is difficult. Hence, to confidently estimate the background, the prediction is mainly based on data-driven methods. The background in the SR

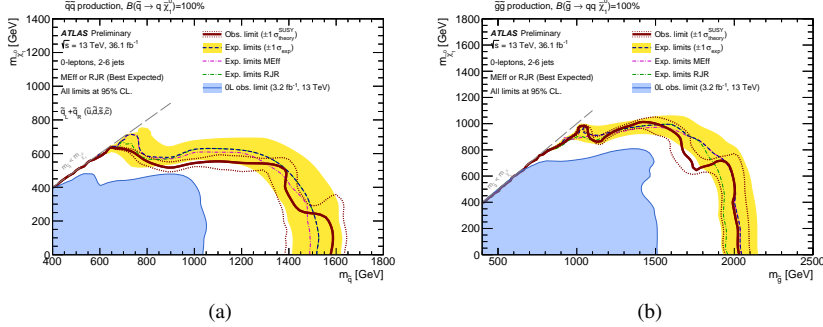


Figure 5: Exclusion limits for (a) light-flavor squark pair-production with direct decay and (b) gluino pair-production with direct decay from the 0-lepton (2–6jets) analysis [9]. Expected limits from Meff- and R-jigsaw-based searches separately are shown. Results are compared with the observed limits obtained by the previous ATLAS searches with the 0-lepton (2–6jets) analysis [21].

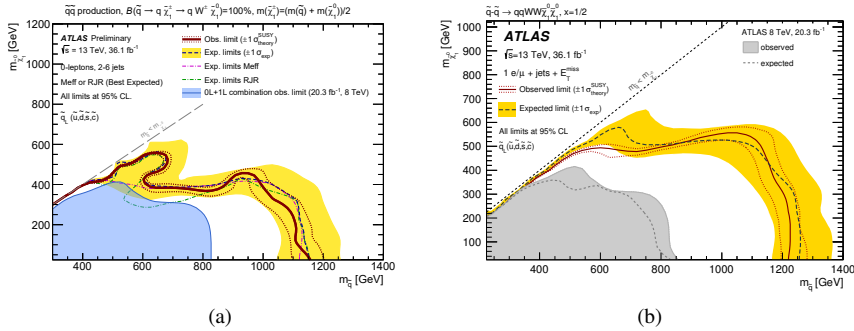


Figure 6: Exclusion limits for light-flavor squark pair-production with one-step decay obtained from (a) 0-lepton (2–6jets) analysis [9] and from (b) 1-lepton analysis [16]. Results are compared with the observed limits obtained by the previous ATLAS searches with combination of the 0-lepton and 1-lepton analysis [22].

is predicted by extrapolating in 2 dimensional plane of a specific variable X and jet multiplicity. In the 0-lepton (7–11jets) analysis, X is $E_T^{\text{miss}} / \sqrt{H_T}$, where H_T is the scalar sum of all jet p_{T} s. In the 1-lepton (9jets) analysis, X is the transverse mass, m_T . m_T is defined from the lepton transverse momentum \mathbf{p}_T^ℓ and the transverse missing momentum, $\mathbf{p}_T^{\text{miss}}$ as

$$m_T = \sqrt{2p_T^\ell E_T^{\text{miss}} (1 - \cos[\Delta\phi(\mathbf{p}_T^\ell, \mathbf{p}_T^{\text{miss}})]}, \quad (1)$$

where $\Delta\phi(\mathbf{p}_T^\ell, \mathbf{p}_T^{\text{miss}})$ is the azimuthal angle between \mathbf{p}_T^ℓ and $\mathbf{p}_T^{\text{miss}}$. m_T can discriminate between signals and W -jets or semi-leptonic $t\bar{t}$ backgrounds because m_T has an upper end-point at the W mass in these backgrounds. In this estimation, it's assumed that the specific variable's distribution is approximately invariant under changes in the jet multiplicity requirements. This assumption is found to be valid

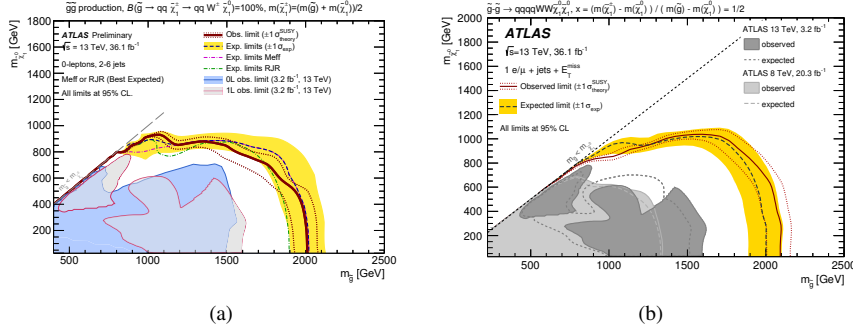


Figure 7: Exclusion limits for gluino pair-production with one-step decay obtained from (a) the 0-lepton (2–6 jets) analysis [9] and from (b) the 1-lepton analysis [16]. Results are compared with the observed limits obtained by the previous ATLAS searches with the 0-lepton analysis [21] and the 1-lepton analysis [23].

when tight m_{eff} requirements as used in this analysis are applied such that the overall activity in the calorimeter and thus the missing transverse energy resolution are not significantly affected by variations in the jet multiplicity. Exclusive control regions $\text{CR}_{A,B,C}$ are defined in this X - N_{jet} 2 dimensional plane as shown in Figure 8, where CR_A is located at high- X and low- N_{jet} , CR_B at low- X and low- N_{jet} , and CR_C at low- X and high- N_{jet} . Based on these regions the background in the high- X -high- N_{jet} signal region can then be estimated with the following equation

$$\frac{N_{\text{CR}_A}}{N_{\text{CR}_B}} = \frac{N_{\text{SR}}}{N_{\text{CR}_C}} \quad \rightarrow \quad N_{\text{SR}}^{\text{est}} = \frac{N_{\text{CR}_A}}{N_{\text{CR}_B}} N_{\text{CR}_C}, \quad (2)$$

where $N_{\langle \text{region} \rangle}^{\text{est}}$ is the (estimated) number of events in a given region.

3.2 Results and interpretation

The background-only fit results in the 0-lepton (7–11 jets) analysis are shown in Figure 9, and the result in the 1-lepton (9 jets) analysis is shown in Figure 4b. No significance excess is observed in the both cases. Then, the model-dependent fits are performed for the signal benchmark models. In the 0-lepton analysis, the limits are obtained by using the SR with the best expected sensitivity at each mass point. In the 1-lepton analysis, the limits are obtained by a model-dependent fit over all of the 9 jets SRs. Figure 10 shows interpretations on the 2 dimensional mass plane of gluino pair-production in a scenario of pMSSM model. Figures 11 shows interpretations on the 2 dimensional mass plane of gluino pair-production with two-step decay in simplified models. In pMSSM scenario, the gluino mass is excluded up to 1.6 TeV, and in two-step decay case the mass is excluded up to around 1.8 TeV.

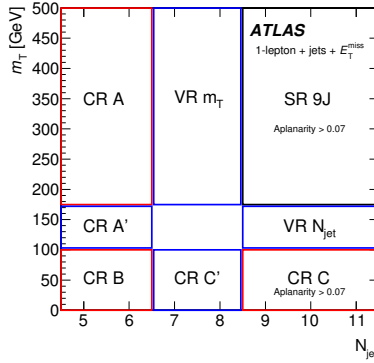


Figure 8: An example of data-driven background-estimation method used in the 1-lepton (9 jets) analysis. Control regions, $CR_{A,B,C}$, are used to estimate background event yields in SR as in Eq. 2. VR m_T and VR N_{jet} are validation regions, and $CR_{A'}$ and $CR_{C'}$ are regions used to estimate background event yield in the validation regions.

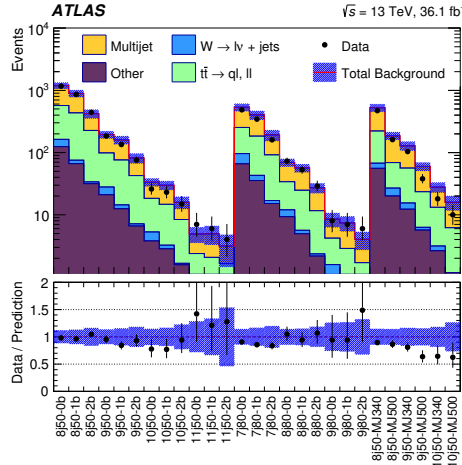


Figure 9: Comparison of the observed data and predicted background event yields in signal regions of the 0-lepton (7–11 jets) analysis [13]. Each bin indicates yields in one signal or validation region. The bottom panel shows the ratio of observed data yields to the total predicted background yields.

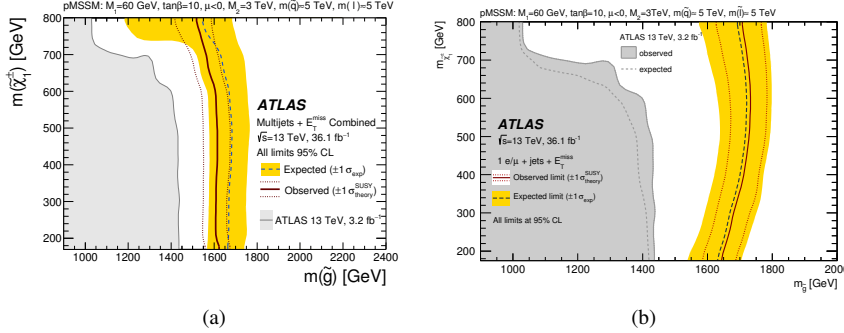


Figure 10: Exclusion limits for gluino pair-production in a scenario of pMSSM model obtained from (a) the 0-lepton (7-11 jets) analysis [13] and from (b) 9-jets signal regions of the 1-lepton analysis [16]. In this pMSSM scenario, $M_1 = 60 \text{ GeV}$, $\tan\beta = 10$, $\mu < 0$, $M_2 = 3 \text{ TeV}$, the squark mass= 5 TeV and the slepton mass= 5 TeV are assumed. X-axis and y-axis indicate masses of gluino and chargino appearing in the decay chain. Results are compared with the observed limits obtained by the previous ATLAS searches with the 0-lepton analysis [24] and the 1-lepton analysis [23].

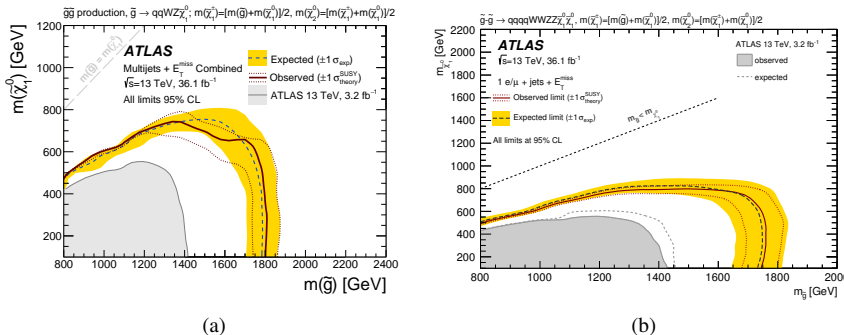


Figure 11: Exclusion limits for gluino pair-production with two-step cascade decay obtained from (a) the 0-lepton (7-11 jets) analysis [13] and from (b) 9-jets signal regions of the 1-lepton analysis [16]. and the result is compared with the observed limits obtained by the previous ATLAS searches with the 1-lepton analysis [23].

4 Multi-*b* analysis

The multi-*b* analysis specially requires at least three *b*-quark jets and the procedure of background estimation is similar to analysis described in Section 2.1. The SM background estimations are performed by using control regions defined for each of the SRs to normalize the background MC simulation.

4.1 Results and interpretation

The results of background-only fits are shown in Figure 12, where no significant excess in data is observed. In the absence of a significant excess, exclusion limits are set by the model-independent fits. Here, multi-bin fits over the signal regions defined to exclude the signals are performed, where the definitions of the SRs are different from the SRs used in Figure 12 in order to maximise signal exclusion limit. The exclusion limits are shown in Figure 13. The assumed signals are gluino-pair production decaying to the LSP via off-shell stop or sbottom. The gluino mass in the signals is excluded up to 1.9–2.0 TeV.

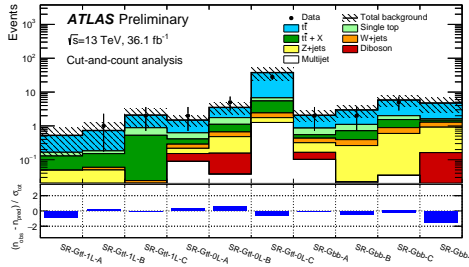


Figure 12: Comparison of the observed data and predicted background event yields in the SRs in the multi-*b* analysis [17]. Each bin indicates yields in one SR. The bottom panel shows the difference between observed data yields and the total predicted background yields divided by total uncertainties.

5 Conclusion

The ATLAS experiment have various searches for squark and gluino using the 2015+2016 dataset recorded at $\sqrt{s} = 13$ TeV, which require different event topology such as different number of jets in order to cover from direct decay signals to two-step decay signals. In the various searches, there is no significant excess. Thus, exclusion limits are set on 2 dimensional mass planes of gluino or squark and the other SUSY particle appearing in decay chain in a given signal model. The squark mass is excluded up to 1.6 TeV in direct decay signal, and the gluino mass is excluded up to 2 TeV in direct and one-step decays including special cases with multi top- or *b*-quarks in final states by the multi-*b* analysis. Exclusion limits are set not only on the signal models shown here, but also other various signal mass spectra, which are described in the ATLAS publications [9, 13, 16, 17].

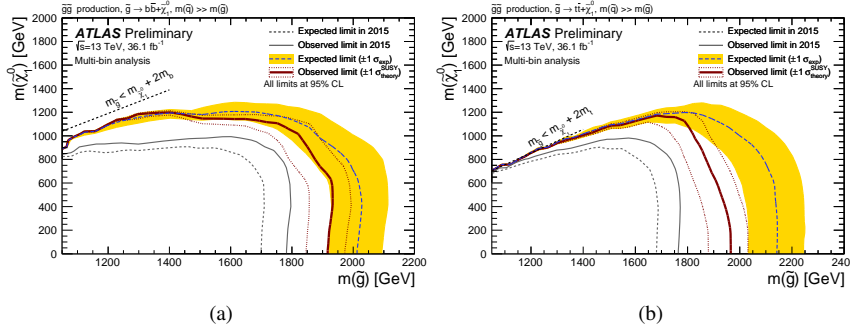


Figure 13: Exclusion limits for gluino pair-production with direct decay to (a) neutralino and bottom quarks via virtual sbottoms and (b) neutralino and top quarks via off-shell stops [17]. Results are compared with the observed limits obtained by the previous ATLAS searches with the multi-*b* analysis [25].

References

- [1] Y.A. Golfand, E.P. Likhtman, *JETP Lett.* **13**, 323 (1971)
- [2] D.V. Volkov, V.P. Akulov, *Phys. Lett. B* **46**, 109 (1973)
- [3] J. Wess, B. Zumino, *Nucl. Phys. B* **70**, 39 (1974)
- [4] J. Wess, B. Zumino, *Nucl. Phys. B* **78**, 1 (1974)
- [5] S. Ferrara, B. Zumino, *Nucl. Phys. B* **79**, 413 (1974)
- [6] A. Salam, J.A. Strathdee, *Phys. Lett. B* **51**, 353 (1974)
- [7] G.R. Farrar, P. Fayet, *Phys. Lett. B* **76**, 575 (1978)
- [8] ATLAS Collaboration, *Journal of Instrumentation* **3**, S08003 (2008)
- [9] ATLAS Collaboration (2017), ATLAS-CONF-2017-022
- [10] J. Alwall, M. Le, M. Lisanti and J. G. Wacker, *Phys. Lett. B* **666**, 34 (2008)
- [11] J. Alwall, P. Schuster, N. Toro, *Phys. Rev. D* **79**, 075020 (2009)
- [12] D. Alves et al., *J. Phys. G: Nucl. Part. Phys.* **39**, 105005 (2012)
- [13] ATLAS Collaboration (2017), [arXiv:1708.02794\[hep-ph\]](https://arxiv.org/abs/1708.02794)
- [14] A. Djouadi et al. (MSSM Working Group) (1998), [arXiv:hep-ph/9901246](https://arxiv.org/abs/hep-ph/9901246)
- [15] C.F. Berger, J. S. Gainer, J. Hewett and T. G. Rizzo, *JHEP* **02**, 023 (2009)
- [16] ATLAS Collaboration (2017), [arXiv:1708.08232\[hep-ph\]](https://arxiv.org/abs/1708.08232)
- [17] ATLAS Collaboration (2017), ATLAS-CONF-2017-021
- [18] M. R. Buckley, J. D. Lykken, C. Rogan and M. Spiropulu, *Phys. Rev. D* **89**, 055020 (2014)
- [19] P. Jackson, C. Rogan, M. Santoni, *Phys. Rev. D* **95**, 035031 (2017)
- [20] P. Jackson, C. Rogan (2017), [arXiv:1705.10733\[hep-ph\]](https://arxiv.org/abs/1705.10733)
- [21] ATLAS Collaboration, *The European Physical Journal C* **76**, 392 (2016)
- [22] ATLAS Collaboration, *Journal of High Energy Physics* **2015**, 54 (2015)
- [23] ATLAS Collaboration, *The European Physical Journal C* **76**, 565 (2016)
- [24] ATLAS Collaboration, *Physics Letters B* **757**, 334 (2016)
- [25] ATLAS Collaboration, *Phys. Rev. D* **94**, 032003 (2016)